MHD Unsteady Incompressible Nanofluid In A Permeable Channel With Suction And Injection

Prathiba. S.R
Shrimathi Devkunvar Nanalal Bhatt Vaishnav College for Women, Chennai,, India

Abstract

An oscillatory incompressible nano fluid past a porous channel was discussed by considering one wall is cold and the another wall is heated. The fluid is electrically conducting nano fluid. Suction is measured at the cold wall and the injection is take place at the heated wall. Oscillatory pressure gradient is present transversely the wall. Heat and mass transfer effects with suction and injection for various parameters along with velocity profile, temperature profile and concentration profile were analyzed with graphs.

1 Introduction

Oscillatory flow in porous media has gained importance lately since of its extensive variety of usages in industry and geophysical applications. With a vast array of potential applications, it is fairly evident that a lot of people have put in their minds and thoughts, trying to invent more innovations in this prevalent field [1].

The phenomenon of hotness and mass transmission in permeable medium has fascinated many investigators. The learning of such streams was introduced by Lighthill [4]. He analyzed the properties of unrestricted stream fluctuations on the movement of a viscid incompressible fluid through an endless platter. Radiation results on instable flow of a nano fluid in an unlimited upright plate was discussed by Mohankrishna, Sugunamma and Sandeep [8].

Misra and Adikary [7] have analyzed the chemical reaction in MHD oscillatory flow with heat and mass transfer effects. An exact solution of an magneto hydro dynamic oscillatory flow through a porous medium in sphere was discussed by Loganathan and Prathiba[5]. Many of the researches studied about the wall conductance on the heat transmission feature of hydro magnetic channel streams. The movement of nano fluids in a uneven permeable channel with temperature basis and chemical effect was studied by Ajaz Ahmed Dar [2]. Durga Prasad, Kiran Kumar and Varma [3] analyzed heat and mass transmission with radiation absorption for MHD current of nanofluid.

Oscillatory flow through many objects has gained importance lately since it is used in industry and geophysical applications. With a vast array of potential applications, it is fairly evident that a lot of people have put in their minds and thoughts, trying to invent more innovations in this prevalent field[6],[9]. Nano particles have introduced to upsurge the transfer of heat in the liquefied. Many methods are used to progress current of the fluids by dangling nano particles in waters. Sasikumar et al.[10] studied the chemical reaction on the result of suction and injection in MHD oscillating current. The same work can be carried out by Verma and Gupta [11] for other parameters.

Recently the movement of nanofluids in a permeable channel was studied by many researchers. In this paper the heat and mass transfer, chemical effect on MHD oscillating flow of nano fluid through porous medium with suction and injection channel is analyzed. The nano fluid effects in velocity contour, temperature profile and concentration profile for various parameters are discoursed. Heat and mass transfer of several parameters are analyzed.

2 Governing equations

Oscillatory electrically conducting nano fluid with the viscous incompressible movement in a channel bounded by the porous medium with suction and injection is considered. Here suction is considered at the cold wall and the injection is take place at the heated wall. Oscillatory pressure gradient is present transversely the wall, so the subsequent flow is instable.

Let x axis be the channel wall and y axis is horizontal to the flow. Nano fluid is inserted over the heated wall and the fluid is sucked through the cold wall.

T_0 and $T$are the temperature of the two walls. Magnetic effect is applied normal to the walls. Nano fluid is moving with the constant velocity u_0.

The governing equation of the nano fluid flow are given by

$$\rho_{nf}\left(\frac{\partial u}{\partial t}\right)-\rho_{nf}u_0\left(\frac{\partial u}{\partial y}\right)=-\frac{\partial p}{\partial x}+\mu_{nf}\frac{\partial^2 u}{\partial y^2}-\sigma B_0^2 u-\frac{\mu_{nf}}{K}u$$
$$+(\rho\beta_T)_{nf}g(T-T_0)+(\rho\beta_C)_{nf}g(C-C_0) \qquad (1)$$

$$\left(\rho C_p\right)_{nf}\left[\frac{\partial T}{\partial t}-u_0\left(\frac{\partial T}{\partial y}\right)\right]=K_{nf}\frac{\partial^2 T}{\partial y^2}-\frac{\partial q}{\partial y} \qquad (2)$$

$$\frac{\partial C}{\partial t}-u_0\left(\frac{\partial C}{\partial y}\right)=D\frac{\partial^2 C}{\partial y^2}-K_r^*(C-C_0) \qquad (3)$$

where u - velocity componets along x axis. ρ_{nf} - nanofluid density , μ_{nf} - nanofluid viscosity , σ - electric conductivity of the fluid, B_0 - uniform magnetic field, g - acceleration due to gravity, $(\beta_T)_{nf}$ - coefficient of thermal expansion of nanofluid,$(\beta_C)_{nf}$ - coefficient of mass expansion of nanofluid, T - temperature of the nanofluid, T_0- temperature , C - concentration of the nanofluid, C_0 - concentration, $\left(\rho C_p\right)_{nf}$ - heat capacity of the nanofluid, k - permeable parameter, q - radiative heat flux, K_r^* - chemical reaction parameter and D - mass diffusion coefficient.

Here

$$\frac{\partial q}{\partial y}=4\alpha^2(T_0-T) \qquad (4)$$

Pressure gradient be

$$-\frac{\partial P}{\partial x}=\lambda e^{int'} \qquad (5)$$

where n - frequency of oscillation.

Boundary conditions are

$$y = 0: u = \frac{\sqrt{k}}{\alpha}\frac{du}{dy}, T = T_0, C = C_0 \tag{6}$$

$$y = h: u = 0, T = T_1, C = C_1 \tag{7}$$

The non dimensional quantities are

$$u' = \frac{hu}{\nu},\ x' = \frac{x}{h}, y' = \frac{y}{h}, t' = \frac{\nu t}{h^2}, s^2 = \frac{1}{D_a}, D_a = \frac{K_f}{h^2}, K_r = \frac{h^2 K_r^*}{\nu}, M^2 = \frac{\sigma {B_0}^2 h^2}{\mu_f},$$
$$G_r = \frac{g(\beta_T)_f h^3(T_1 - T_0)}{{\nu_f}^2}, G_c = \frac{g(\beta_c)_f h^3(C_1 - C_0)}{{\nu_f}^2}, p' = \frac{\rho_{nf} p h^2}{{\mu_f}^2}, P_r = \frac{\nu(\rho C_p)_{nf}}{K}, \quad S_c = \frac{1}{D},$$
$$s = \frac{u_0 h}{\nu_f},\ \ N = \frac{4\alpha^2 h^2}{(\rho C_p)_{nf}\,\nu_f}, \theta = \frac{(T - T_0)}{(T_1 - T_0)}, \phi = \frac{(C - C_0)}{(C_1 - C_0)} \tag{8}$$

where U - mean flow velocity, G_r-Grashof number, G_m-modified Grashof number, R_e-Reynolds number, P_e-Peclet number, D_a- Darcy number, M -Hartmann number r , K_r chemical reaction parameter, N is radiation parameter and S_c-Schmidt number.

Using the non dimensional terms

$$\frac{\partial u'}{\partial t'} - s\frac{\partial u'}{\partial y'} = \lambda e^{int'} + \frac{\partial^2 u'}{\partial y'^2} + G_r\theta + G_C\phi - (\frac{1}{D_a} + M^2)u' \tag{9}$$

$$\frac{\partial \theta}{\partial t'} - s\frac{\partial \theta}{\partial y'} = \frac{\partial^2 \theta}{\partial y'^2} + N\theta \tag{10}$$

$$\frac{\partial \phi}{\partial t'} - s\frac{\partial \phi}{\partial y'} = \frac{1}{S_c}\frac{\partial^2 \phi}{\partial y'^2} - K_r\phi \tag{11}$$

The corresponding non dimensional boundary conditions are

$$u' = \beta\frac{du'}{dy'}, \theta = 0, \phi = 0 \quad \text{at } y' = 0 \tag{12}$$

$$u' = 0, \theta = 1, \phi = 1 \quad \text{at } y' = 1 \tag{13}$$

3 Method of Solutions

Finding solutions for the equations (9)-(11) assume

$$u(y', t') = u_0(y')e^{int'} \tag{14}$$

$$\theta(y', t') = \theta_0(y')e^{int'} \tag{15}$$

$$\phi(y', t') = \phi_0(y')e^{int'} \tag{16}$$

Equations (9)-(11) becomes

$$\frac{d^2u_0}{dy'^2}+\frac{du_0}{dy'}-\left(in+M^2+\frac{1}{D_a}\right)u_0=-(G_r\theta_0+G_C\phi_0-\lambda) \tag{17}$$

$$\frac{d^2\theta_0}{dy'^2}+sP_r\frac{d\theta_0}{dy'}+(NP_r-P_r in)\theta_0=0 \tag{18}$$

$$\frac{d^2\phi_0}{dy'^2}+s\,S_c\frac{d\phi_0}{dy'}+(K_r+in)S_c\phi_0=0 \tag{19}$$

And the boundary conditions are

$$u_0=\beta\frac{du'}{dy'},\theta_0=0,\phi_0=0 \quad \text{at } y=0 \tag{20}$$

$$u_0=0,\theta_0=1,\phi_0=1 \quad \text{at } y=1 \tag{21}$$

Solving (17)-(19)along with the boundary conditions (20) and (21), then

$$u_0=A_1e^{E_1y'}+A_2e^{E_2y'}-A_7+\frac{G_r}{e^{E_3}-e^{E_4}}\left(e^{E_3y'}-e^{E_4y'}\right)e^{int'}+\frac{G_C}{e^{E_5}-e^{E_6}}\left(e^{E_5y'}-e^{E_6y'}\right)e^{int'} \tag{22}$$

$$\theta_0=\frac{1}{e^{E_3}-e^{E_4}}\left(e^{E_3y'}-e^{E_4y'}\right) \tag{23}$$

$$\varphi_0=\frac{1}{e^{E_5}-e^{E_6}}\left(e^{E_5y'}-e^{E_6y'}\right) \tag{24}$$

Using equations (20) –(21), then equations (22)-(24) becomes

$$u=\left[A_1e^{E_1y'}+A_2e^{E_2y'}-A_7+\frac{G_r}{e^{E_3}-e^{E_4}}\left(e^{E_3y'}-e^{E_4y'}\right)e^{int'}+\frac{G_C}{e^{E_5}-e^{E_6}}\left(e^{E_5y'}-e^{E_6y'}\right)e^{int'}\right]e^{int'} \tag{25}$$

$$\theta=\left[\frac{1}{e^{E_3}-e^{E_4}}\left(e^{E_3y'}-e^{E_4y'}\right)\right]e^{int'} \tag{26}$$

$$\phi=\left[\frac{1}{e^{E_5}-e^{E_6}}\left(e^{E_5y'}-e^{E_6y'}\right)\right]e^{int'} \tag{27}$$

4 Shear Stress

The shear stress is

$$S=-\frac{\partial u}{\partial y'}$$

$$S=-\left[A_1E_1e^{E_1y'}+A_2E_2e^{E_2y'}+A_3E_3e^{E_3y'}+A_4E_4e^{E_4y'}+A_5E_5e^{E_5y'}+A_6E_6e^{E_6y'}\right]e^{int'} \tag{28}$$

5 Heat Transfer

The rate of heat transfer

$$Nu = -\frac{\partial\theta}{\partial y'}$$

$$Nu = -\left[B_1(E_3 e^{E_3 y'} - E_4 e^{E_4 y'})\right]e^{int'} \quad (29)$$

6 Mass Transfer

The rate of mass transfer

$$Sh = -\frac{\partial\phi}{\partial y'}$$

$$Sh = -\left[B_3\ (e^{E_5 y'} - e^{E_6 y'})\right]e^{int'} \quad (30)$$

7 Results and Discussion

The various parameter of the nanofluid past oscillatory channel is discussed. The velocity profile for various parameters are studied using different values. The results are obtained for the flows by using the Fig.1 to Fig.21.Velocity profiles are exposed in Fig.1 to Fig.8. In Fig.1velcity growths for growing values of the parameter M and with the remaining parameters are Gc=1, N=1,s=2, Sc=0.6, Pr=1, λ=1, Gr=2 and Kr=1.From Fig.2, it is realized that the velocity gradually declines with growing Grashof number with the remaining parameters Gc=1, N=1, s=2, Sc=0.6, Pr=1, λ=1, M=1 and Kr=1.

For increasing Pr the velocity becomes decreases for some radius , after certain period it is steadily growing. These results are present in fig.3and the remaining parameters are same in the previous figure. For increasing N the velocity becomes increases steadily. These results are existing in fig.4 and the parameters are Gc=1, M=1, s=2, Sc=0.6, Pr=1, λ=1, Gr=2 and Kr=1. The behavior of modified Grashof number in velocity profile is noticeable. Velocity increases for modified Grashof number and the variation are large. That is shown in Fig.5.

For Schmidt number the velocity profile raises for particular y, after that it is slowly cuts that is in fig.6. When a graph is plotted between velocity and radial distance of the channel , (Fig.7) velocity rises with increase chemical reactor parameter. Fig.8 represents velocity profile for several data of the suction parameter. Here velocity profile shrinkages with increasing s and the remaining parameters are Gc=1, M=1, N=2, Sc=0.6, Pr=1, λ=1, Gr=2 and Kr=1. Velocity profile is plotted for various values of the positive constant λ, that is presented in fig.9. For increasing values of λ velocity increases slowly and after certain value of y, it suddenly raises then it naps.

Temperature profiles are represented in Fig.10 to Fig.12. From Fig.10, we see that there is noteworthy change for different values of N, whenever N increases the temperature raises. Temperature decreases for increasing Prantal number and the rate of decrement is in Fig.11.Then for higher y, a slight slope is in the temperature. For positive values of s temperature declines for increasing of the suction parameter and the remaining parameters are Pr=1, Gc=1, Sc=0.6, M=1, Gr=2, N=1,Kr=1 that is in Fig.12.

. Concentration profile is studied from Fig.13 to Fig.18. In Fig.13 concentration is decreases and tends to a single value for different increasing value of the chemical reaction parameter. If a graph is designed against concentration to t (Fig.14) in the occurrence of a permeability and magnetic parameter, the increase rate of t leads to the concentration to decrease. In Fig.15. concentration diminutions for growing numbers of positive Schmidt number, with Gc=1, M=1, N=2, Pr=1, λ=1, Gr=2 and Kr=1. Concentration reduces as the values of suction parameter rises and s reaches a single value for some y is presented in Fig.16. The behavior of concentration profile is slightly different for different n. It gradually decreases for growing values of n is presented in Fig.17.

The proportion of heat transfer is denoted in Fig.18 and Fig.19. As understood in Fig.18, heat transfer raises as the radiation parameter upsurges with Pr=1, Gc=1, Sc=0.6, M=1, Gr=2,Kr=1. Again, for the varying suction parameter rate of heat transfer decreases gradually, as represented in Fig.19. Shear stress is represented in Fig.20 and Fig.22. As seen in Fig.20, initially skin friction increases for increasing modified Grashof number but for higher values of y it decreases. And, for the varying Grashof number,, shear stress increases, for higher values the raise in , shear stress is very high as represented in Fig.21. Once a chart is designed for different values of suction parameter (Fig.22), shear stress declines as the suction parameter rises with Pr=1, Sc=0.6, M=1, Gr=2, N=1,Kr=1.

8 Conclusion

When the flow is through the porous channel, the velocity profile is analyzed for varying radiation parameter, suction parameter, magnetic parameter, Grashof numbers , Prandtl numbers and Schmidt numbers. Velocity profile increases varying Hartman number, radiation parameter, modified Grashof number, Schmidt number , chemical reaction parameter and the positive constant and decreases for Grashof number, Prandtl number and suction parameter.

Temperature profile is studied for radiation parameter, Prandtl number and suction (injection) parameter. Temperature profile is found to decrease for most of the above said parameters , increases for the radiation parameter. Concentration profile is studied for chemical reaction parameter, Schmidt number, suction (injection) parameter, time values and frequency parameter. The resulting curve decreases for all the above said parameters and mostly reaches a single value.

Shear stress is discussed for modified Grashof number , Grashof number and suction parameter. Other than suction parameter shear stress decreases for remaining values. Heat transfer is analyzed for radiation and suction parameter. It increases for N and decreases for suction parameter.

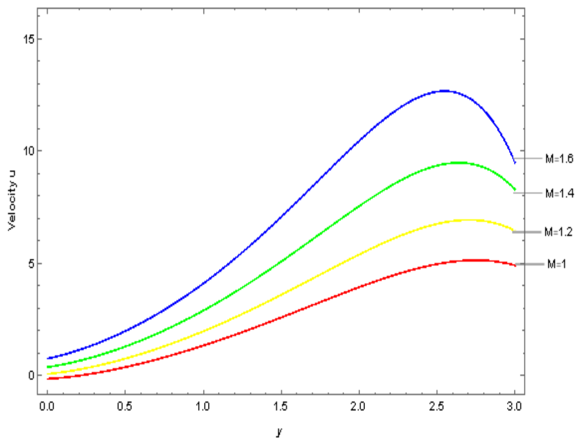

Fig.1 Velocity profile for various values of M with Gc=1, Sc=0.6, Pr=1, Gr=2, s=2, N=1

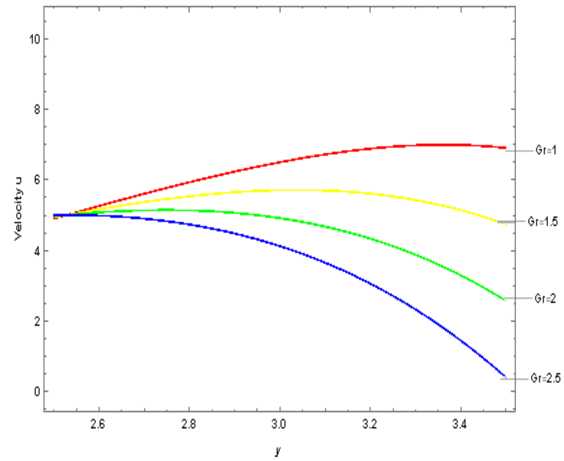

Fig.2 Velocity profile for various values of Gr with Gc=1, Sc=0.6, Pr=1, M=1, s=2, N=1

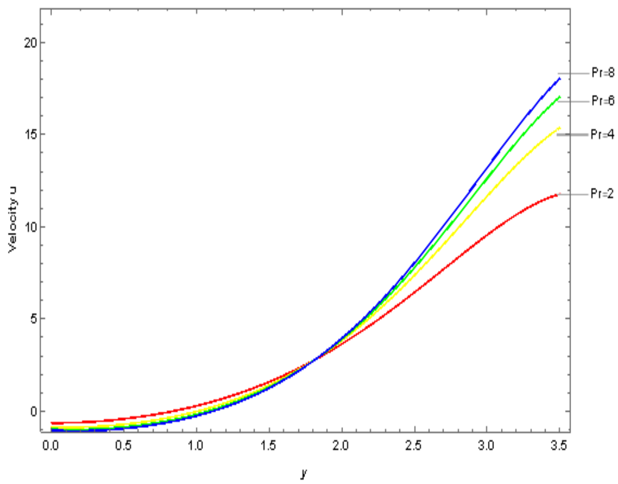

Fig.3 Velocity profile for various values of Pr with Gc=1, Sc=0.6, M=1, Gr=2, s=2, N=1

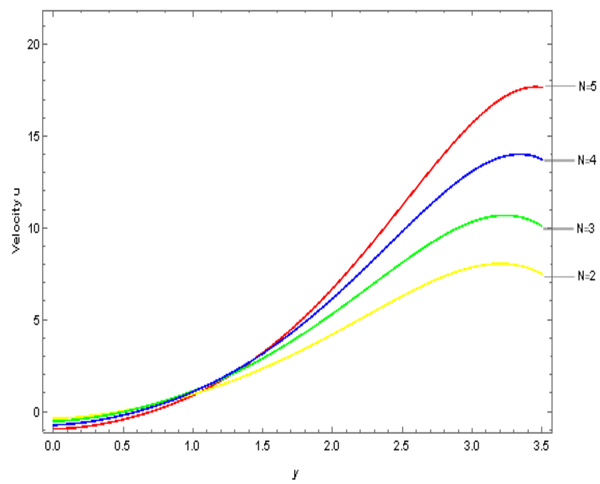

Fig.4 Velocity profile for various values of N with Gc=1, Sc=0.6, M=1, Gr=2, s=2, Pr=1

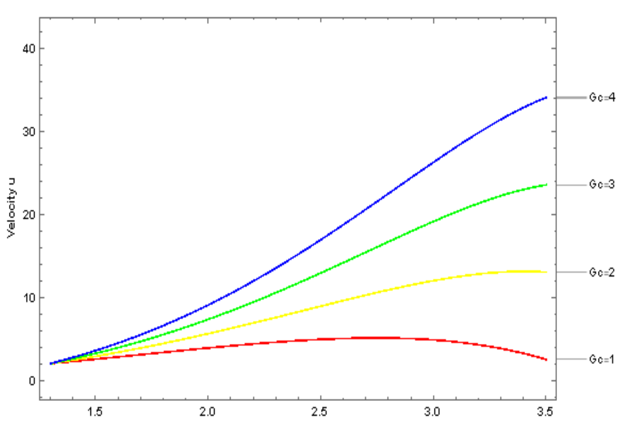

Fig.5 Velocity profile for various values of Gc

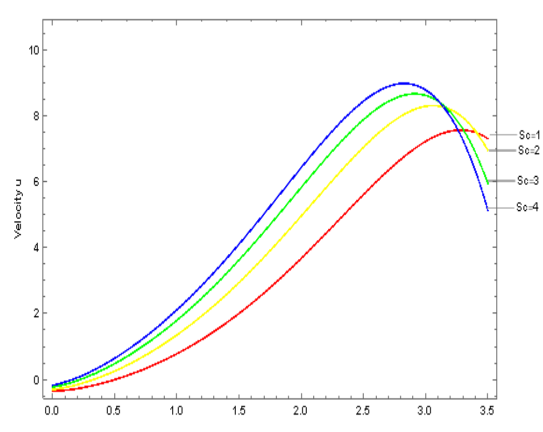

Fig.6 Velocity profile for various values of Sc

with Pr=1, Sc=0.6, M=1, Gr=2, s=2, N=1

with Gc=1, Pr=1, M=1, Gr=2, s=2, N=1

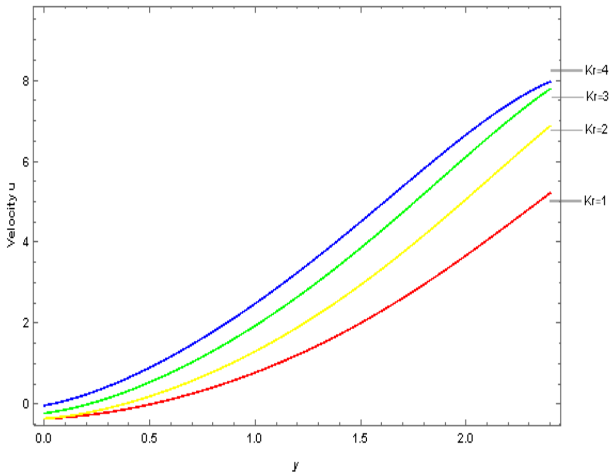

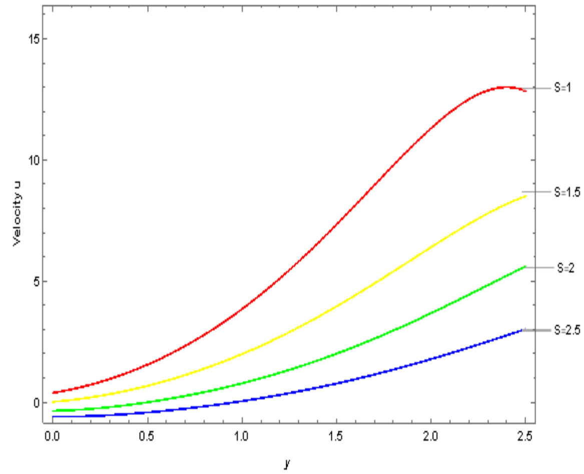

Fig.7 Velocity profile for various values of Kr with Gc=1, Sc=0.6, M=1, Gr=2, s=2, N=1

Fig.8 Velocity profile for various values of s with Gc=1, Sc=0.6, M=1, Gr=2, Pr=1, N=1

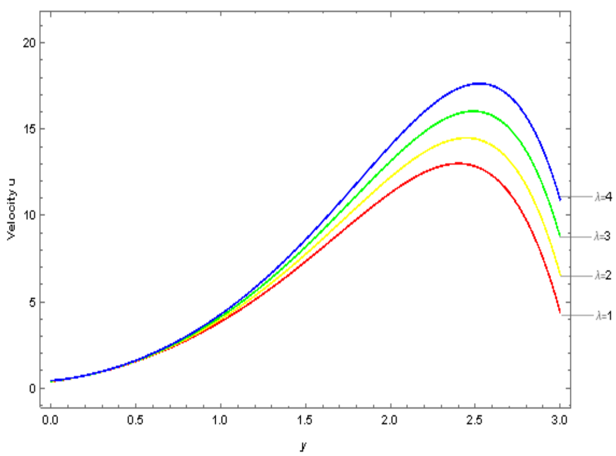

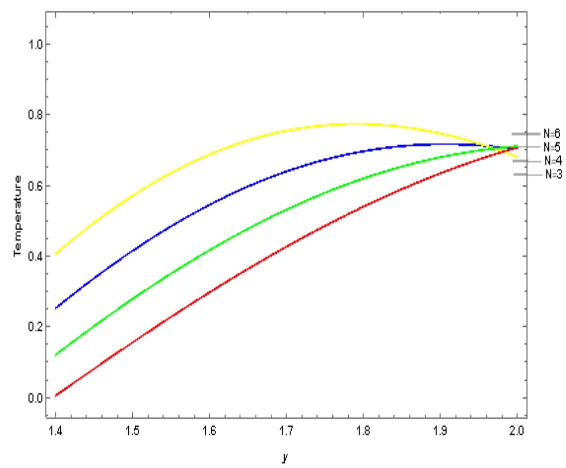

Fig.9 Velocity profile for various values of λ with Gc=1, Sc=0.6, M=1, Gr=2, s=2, N=1

Fig.10 Temperature profile for various values of N with Gc=1, Sc=0.6, M=1, Gr=2, s=2

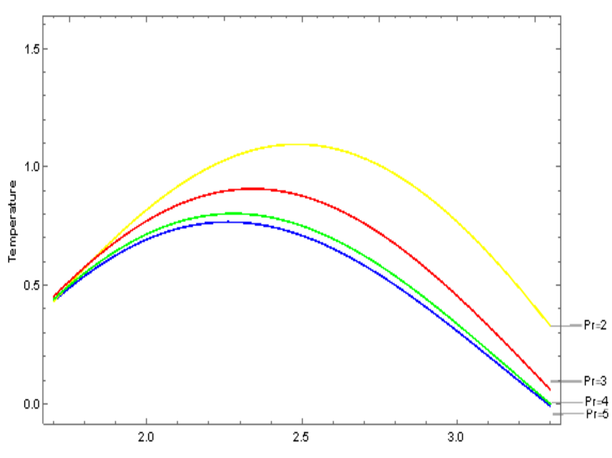

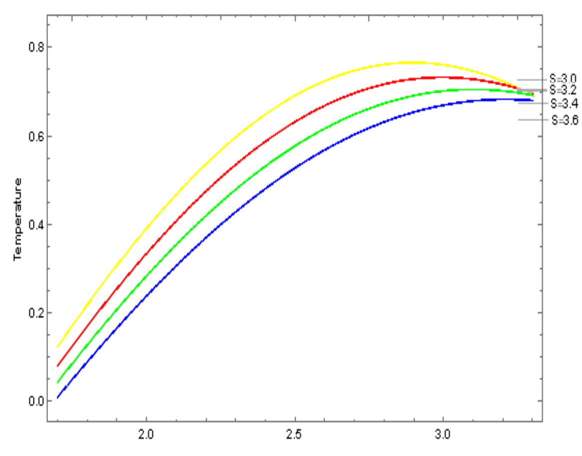

Fig.11 Temperature profile for various values of

Fig.12 Temperature profile for various values of

Pr **with Gc=1, Sc=0.6, M=1, Gr=2, s=2, N=1**

s **with Gc=1, Sc=0.6, M=1, Gr=2, Pr=1, N=1**

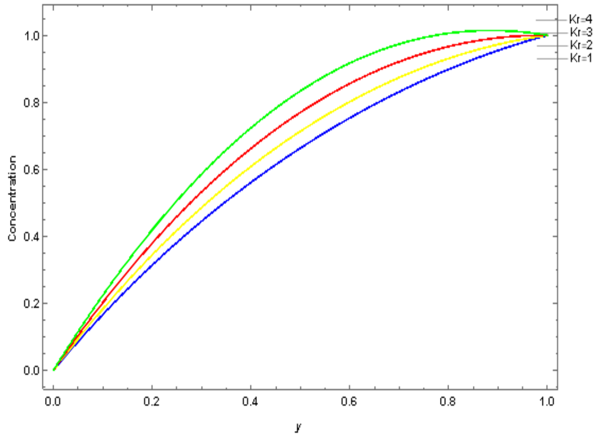

Fig.13 Concentration profile for various values of Kr with Gc=1, Sc=0.6, M=1, Gr=2, s=2, N=2

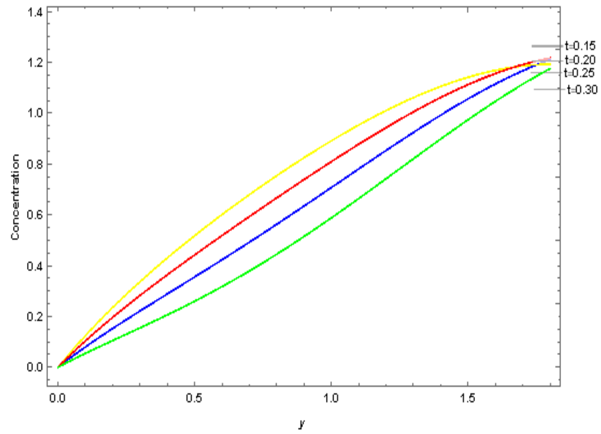

Fig.14 Concentration profile for various values of t with Gc=1, Sc=0.6, M=1, Gr=2, s=2, N=2

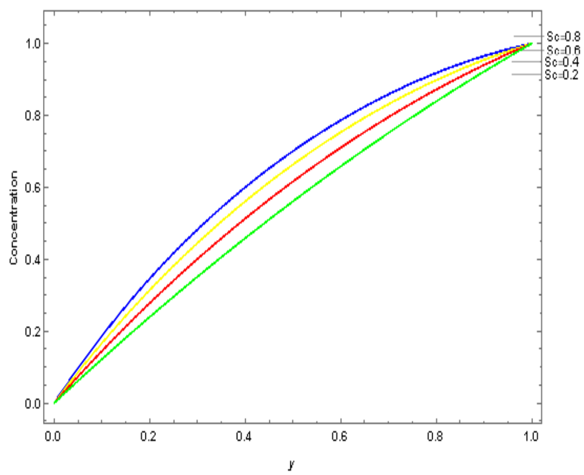

Fig.15 Concentration profile for various values of Sc with Gc=1, Pr=1, M=1, Gr=2, s=2, N=2

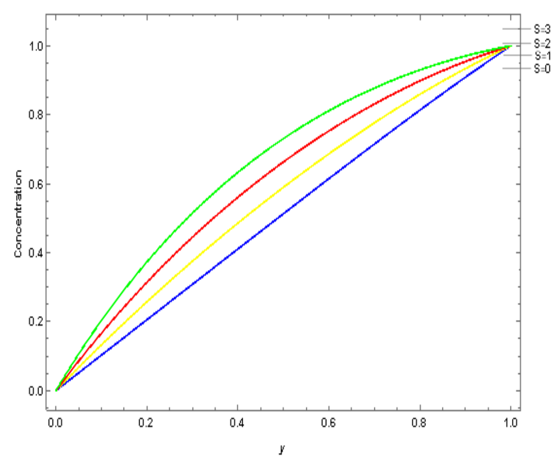

Fig.16 Concentration profile for various values of s with Gc=1, Sc=0.6, M=1, Gr=2, Pr=1, N=2

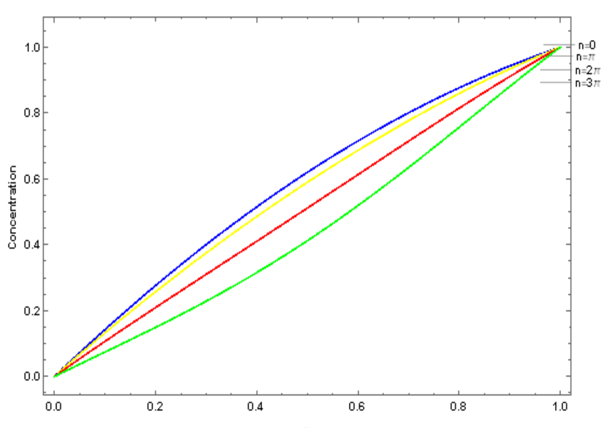

Fig.17 Concentration profile for various values of

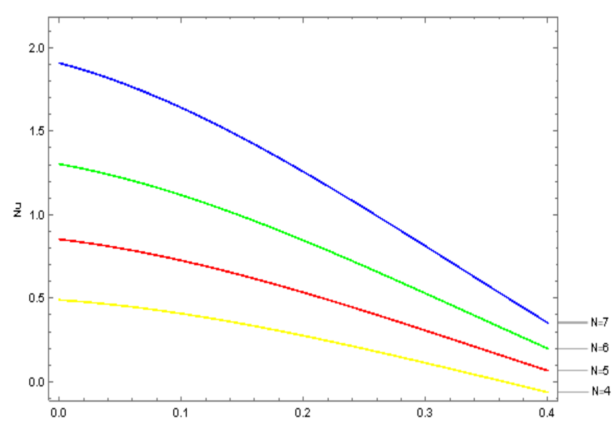

Fig.18 Heat transfer for various values of N

n with Gc=1, Sc=0.6, M=1, Gr=2, s=2, N=2

with Gc=1, Sc=0.6, M=1, Gr=2, s=2, Pr=1

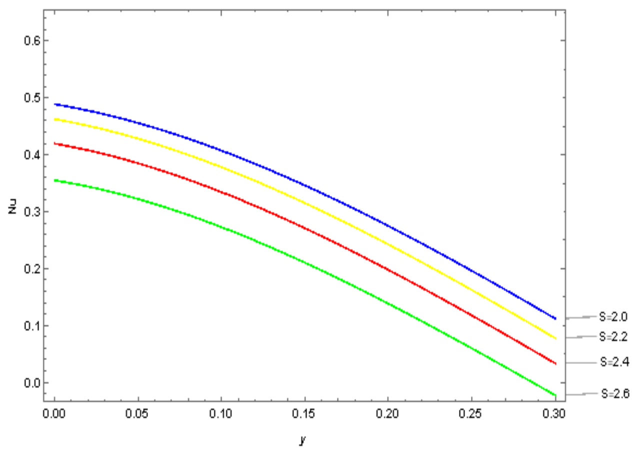

Fig.19 Heat transfer for various values of s with Gc=1, Sc=0.6, M=1, Gr=2, N=2, Pr=1

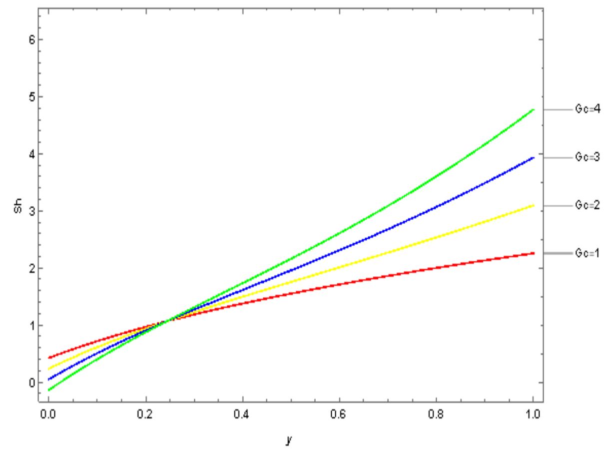

Fig.20 Shear stress for various values of Gc with N=2, Sc=0.6, M=1, Gr=2, s=2, Pr=1

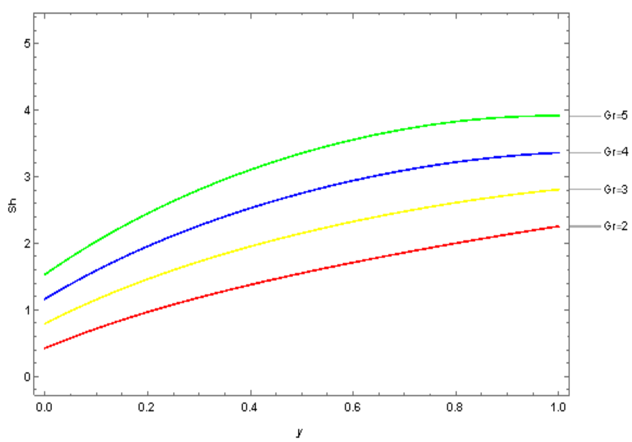

Fig.21 Shear stress for various values of Gr with N=2, Sc=0.6, M=1, Gc=1, s=2, Pr=1

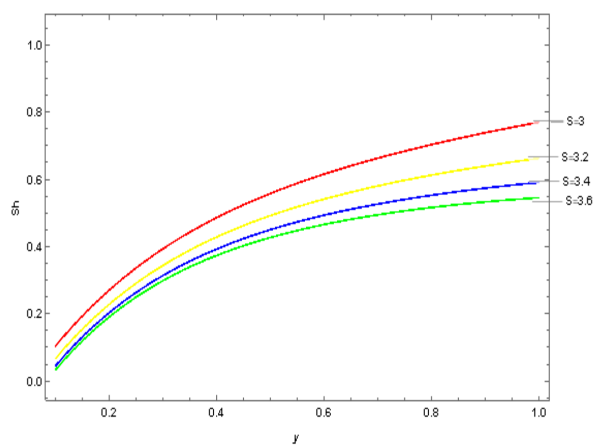

Fig.22 Shear stress for various values of s with N=2, Sc=0.6, M=1, Gr=2, Gc=2, Pr=1

Appendix

$$E_1 = \frac{-s+\sqrt{s+4(in+M^2+\frac{1}{D_a})}}{2}$$

$$E_2 = \frac{-s-\sqrt{s+4(in+M^2+\frac{1}{D_a})}}{2}$$

$$E_3 = \frac{-sP_r+\sqrt{(sP_r)^2-4(N-in)P_r}}{2}$$

$$E_4 = \frac{-sP_r-\sqrt{(sP_r)^2-4(N-in)P_r}}{2}$$

$$E_5 = \frac{-sS_c - \sqrt{(sS_c)^2 - 4(K_r + in)S_c}}{2}$$

$$E_6 = \frac{-sS_c - \sqrt{(sS_c)^2 - 4(K_r + in)S_c}}{2}$$

$$E_7 = A_3 e^{E_3} + A_4 e^{E_4} + A_5 e^{E_5} + A_6 e^{E_6} + A_7$$

$$E_8 = -(A_3 + A_4 + A_5 + A_6 + A_7)$$

$$E_9 = A_3 E_3 + A_4 E_4 + A_5 E_5 + A_6 E_6$$

$$B_1 = \frac{1}{e^{E_3} - e^{E_4}}$$

$$B_2 = \frac{-1}{e^{E_3} - e^{E_4}}$$

$$B_3 = \frac{1}{e^{E_5} - e^{E_6}}$$

$$B_4 = \frac{-1}{e^{E_5} - e^{E_6}}$$

$$A_1 = \frac{E_8 - \beta E_9 + A_2(\beta E_2 - 1)}{(1 - \beta E_1)}$$

$$A_2 = \frac{E_7(1 - \beta E_1) + e^{E_1}(E_8 + \beta E_9)}{\left(e^{E_1} - e^{E_2}\right) + \beta(E_1 e^{E_2} - E_2 e^{E_1})}$$

$$A_3 = \frac{G_r B_1}{{E_3}^2 - sE_{3-}(in + M^2 + \frac{1}{D_a})}$$

$$A_4 = \frac{G_r B_2}{{E_4}^2 - sE_4 - (in + M^2 + \frac{1}{D_a})}$$

$$A_5 = \frac{G_c B_3}{{E_5}^2 - sE_{5-}(in + M^2 + \frac{1}{D_a})}$$

$$A_6 = \frac{G_c B_4}{{E_6}^2 - sE_{6-}(in + M^2 + \frac{1}{D_a})}$$

$$A_7 = \frac{\lambda}{in + M^2 + \frac{1}{D_a}}$$

References

[1] Ahmed. S, Effects of unsteady free convective MHD flow through a porous medium bounded by an infinite vertical porous plate, Bulletin of Calcutta Mathematical Society, 99 , (2007) , 511-522.

[2] Ajaz Ahmad Dar, Effect of an inclined magnetic field on the flow of nanofluids in a tapered asymmetric porous channel with heat source/ sink and chemical reaction, Applied science and Innovative research, 1 (2), (2017), 104-118.

[3] Durga Prasad.P, Kiran Kumar.R.V.M.S.S and Varma.S.V.K, Heat and mass transfer analysis for the MHD flow of nanofluid with radiation absorption, Ain shams Engineering Journal, 9, (2018), 801-813.

[4] Lighthill.M.J, The response of laminar skin-friction and heat transfer to fluctuations in the stream velocity, Proceedings of the Royal Society Ser. A, 224, (1954), 1-23.

[5] Loganathan.C and Prathiba.S.R, Magnetohydrodynamic flow past a porous spherical aggregate with stress jump condition, Progress in Nonlinear Dynamics and Chaos, 1, (2013), 76-92.

[6] Loganathan.C and Prathiba.S.R, Magnetohydrodynamic oscillatory Stokes flow past a porous sphere, Elixir Applied Mathematics, 74, (2014), 26960-26974.

[7] Misra.J.C and Adikary.S.D, MHD oscillatory channel flow, heat and mass transfer in a physiological fluid presence of chemical reaction, Alexandria engineering Journal, 55, (2016), 287-297.

[8] Mohankrishna.P, Sugunamma.V and Sandeep.N, Radiation and magnetic field effects on unsteady natural convection flow of nanofluid past an infinite vertical plate with heat source, Chem. Proc. Eng. Res., 25, (2014), 39-52.

[9] Prathiba.S.R and Sumathi.K, Magnetohydrodynamic flow past a rotating circular cylinder, International Journal of Computer Application, 4(3), (2013), 18-29.

[10] Sasikumar.J, Bhuvaneshwari.S and Govindarajan.A, Diffusion of chemically reactive species in MHD oscillatory flow with thermal radiation in the presence of constant suction and injection, Journal of Physics, 1000, (2018), 1-12.

[11] Verma.V.K and Gupta.A.K, MHD flow in porous channel with constant suction/injection at the walls, International Journal of Pure and Applied Mathematics, 118 (1), (2018), 111-123.